

Behaviour and Design of Reinforced Concrete Beams with Large Openings

Stefan Ehmann & Martina Schnellenbach-Held

Institute of Concrete Structures and Materials, TU Darmstadt, Germany

ABSTRACT: Concrete beams with large openings are often designed in a simple and global way ignoring a lot of important parameters. In order to identify and assess these parameters a comprehensive study using the Finite Element Method with nonlinear material properties simulating an innovative testing scheme has been performed. The main focus lays on openings located in areas with high shear stresses. For such openings little information is available. The presented results will show that the design of beams with large openings can be done in a more reliable way in the future. A practical design concept will be developed which fits the ultimate and the serviceability limit state.

1 INTRODUCTION

Beams with large openings are applied in the structures of almost every building. These openings affect the beams' behaviour in the ultimate and the serviceability limit state. The preponderant number of design concepts (Leonhardt 1977, Eligehausen & Gerster 1993, Wommelsdorf 1993) are based on experimental investigations of the 1960's (Lorentsen 1962, Nasser et al. 1967, Hanson 1969). The point of departure for each method is the distribution of the shear force on the chord members to calculate the secondary moments and combine them with the axial forces.

Much more comprehensive investigations have been done by Mansur & Tan (1999) which led to a completely different design approach. Their observations in their experimental studies could identify significant parameters like the opening length and height, the opening's eccentricity in the beam and the location of the opening. Based on these findings they developed a design concept using the plasticity theory. Mansur & Tan (1999) allow four plastic hinges, one at each chord's end until the beam fails. This method delivers sound information about the ultimate limit state. The serviceability limit state is taken into account by regulations derived from the experimental results.

Up to now only few experimental investigations could manage to examine the behaviour of beams with openings close to the support and in the contraflexure points of statically indeterminate beams. Figure 1 shows a selection of test results which are

included in our database of all available 83 tests worldwide. At this juncture the ratio of the bending moment and the shear force M/V [m] at the opening's midspan represents the distance of the opening to the support in one span beams.

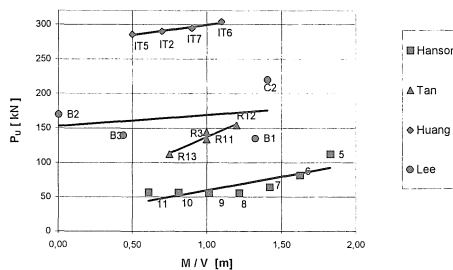


Figure 1. Influence of the opening's location on the ultimate load

2 EXPERIMENTAL PROGRAM

Evaluating the test series in which the opening's location has been varied it is obvious that the ultimate load gets lower with decreasing M/V -ratio. This awareness and the little quantity of tests in that area of high shear stresses led to the recommendation of some authors to dissuade from such openings. However because of practical demands these openings are placed close to the support in many cases.

A proper proposal for a testing scheme free from

geometrical restrictions has been made by Reit (1994). Reit's testing scheme allows to control the magnitude of the internal forces M indicated by P_M and V indicated by P_Q separate from each other. This possibility is very useful to examine single parameters without changing the system. The testing scheme for a beam with an opening is shown in figure 2 while the resulting internal forces are presented in figures 3a-c.

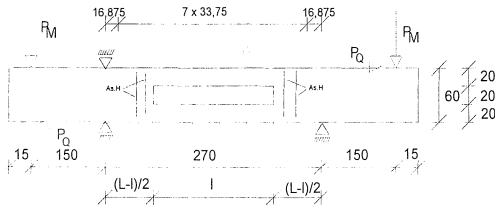


Figure 2: Testing scheme

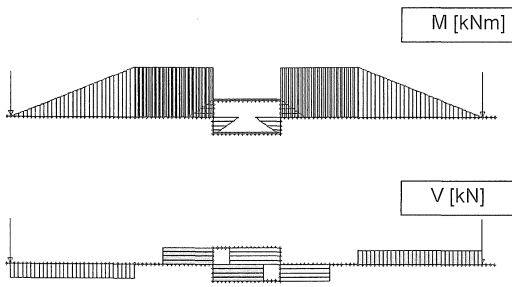


Figure 3a: Internal forces M and V due to P_M

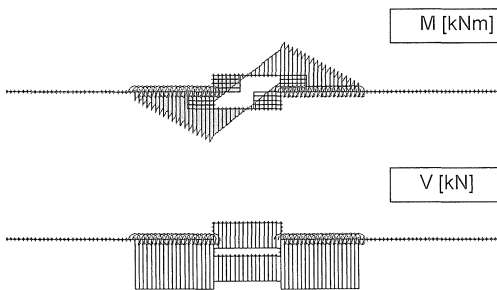


Figure 3b: Internal forces M and V due to P_Q

The following parameters can be examined with this testing scheme within the scope of twelve experiments:

- The length of the opening subjected to high shear stresses.
- Different M/V -ratios.

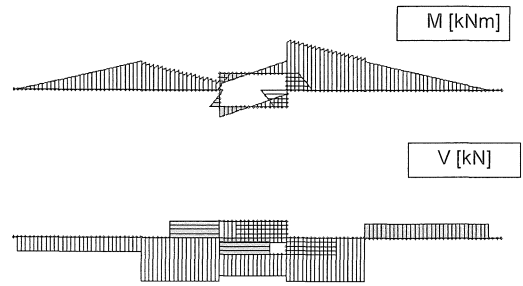


Figure 3c: Internal forces M and V due to P_M and P_Q

- Variations of the quantity of the reinforcement of the chord members.

These parameters have a significant influence on

- the ultimate load and the cause of failure,
- the distribution of the shear force on the chord members and
- the position of the contraflexure point of the chord members, which results in the bending moments at the chords' ends.

With great success some simplified experiments have already been conducted. The preparations for the comprehensive test series will start in the near future.

3 FINITE ELEMENT ANALYSES

Before starting the experiments in our laboratory we examined the testing scheme presented above extensively by using the Finite Element Method with nonlinear material properties. We used the Finite Element program system DIANA. DIANA offers the possibility of a crack model which is based upon the total strain concept. This has been developed along the lines of the Modified Compression Field Theory, originally proposed by Vecchio & Collins (1986). Here the rotating crack model has been selected. The element types are eight-node isoparametric plain stress elements using a full 3×3 Gauß integration scheme. For modelling the longitudinal reinforcement and the stirrups embedded reinforcement bars have been implemented.

The material behaviour of the steel has been described with the law of Dilger (1966) which fits the real behaviour very well. For concrete under tension a parabolic curve has been used and Hordijk's (1992) material law has been applied for the concrete's behaviour under tensile stress. The fracture energy G_F can be derived from the CEB-FIP Model Code (1990).

The FE-model could be verified in several studies (Ehmann et al. 1999) also by analyzing beams with openings tested by Tan (1982). The load-displacement-diagrams for the selected beams R3 ($M/V=1,0$ m) and R10 ($M/V=0,8$ m), tested by Tan, are shown in the following figures 4 and 5. It is obvious that the tensile stress and the fracture energy, which have to be derived from the compression strength, have great influence on the ductility of the beams. Nevertheless the calculated results are in a very proper agreement with the experimental results. Some differences in the stiffness show a typical phenomenon of the smeared cracking concept with totally fixed reinforcement to the concrete elements.

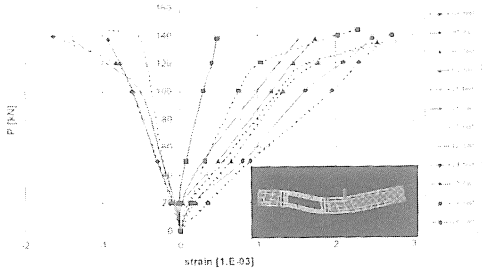


Figure 6. Steel strains of beam R3

because cracks prevent reliable measurements on the concrete's surface. Electric gauges on stirrups can only give reliable measurements if the investigated results can be related to proportion. Here the FE-analysis obviously has great advantages. Figure 7 clarifies that a constant proportion without representing the chords' varying stiffness as proposed by Leonhardt (1979) is not a convinceable approach. A better one is the concept of Eligehausen and Gerster (1993). But it fails in the serviceability limit state because of its discontinuous formulation. Mansur's concept (Mansur & Tan 1999) delivers a good proportion at the ultimate limit state but for lower loadlevels his concept predict a suitable shear force distribution either.

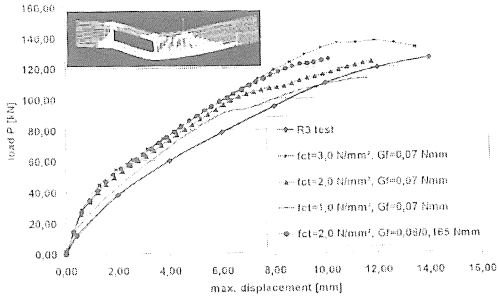
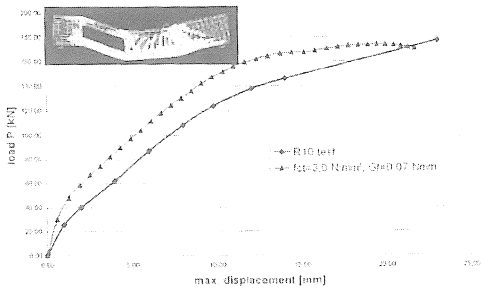


Figure 4. Load-displacement-diagram for R3 (Tan 1982) compared with FE-results



Another very suitable and convinceable check of the FE-results is the comparison of the steel strains. Tan (1982) fixed several gauges to the stirrups and the longitudinal reinforcement. The FE-results approximate the results from the experiment very well (fig. 6).

For the beam R3 the shear force distribution on the chords is shown in figure 7. Comparisons with experimental results are not possible. In the most cases the shear force distribution is not determined

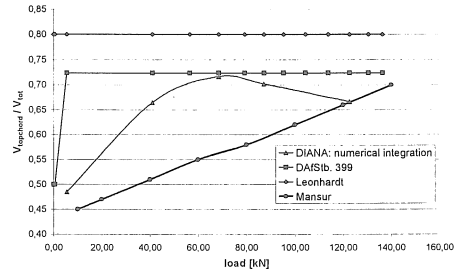


Figure 7. Shear force distribution on the chord of beam R3

4 RESULTS OF THE THEORETICAL STUDIES

The designated experimental investigations have been extended to more than 25 tests in order to study the parameters in more detail. Apart from the opening's location represented by the M/V -ratio from 0,0 m to 1,5 m the reinforcement in the chords has been changed. In the first series the reinforcement quantities of the chord members were fixed to $A_{s2}=A_{s3}=A_{s4}=2,26$ cm² and only the longitudinal reinforcement for the global moment M in the tension chord was varied from $A_{s1}=2,26$ cm² up to $A_{s1}=9,82$ cm². In the second series the chord's reinforcement amounted to $A_{s2}=A_{s3}=A_{s4}=4,02$ cm² and the longitu-

dinal reinforcement for the global moment M in the tension chord was varied again between $A_{s1}=2,26$ cm² and $A_{s1}=9,82$ cm². The parameter of the reinforcement ratio in the tension chord which represents the reinforcement's symmetry is called α_t .

$$\alpha_t = \frac{A_{s2}}{A_{s1} + A_{s2}}; \quad \alpha_t \leq 0,5 \quad (1)$$

These two parameters affect the shear force distribution as well as the contraflexure point of the chords which define the magnitude of the moments in the chord members. Therefore both parameters are responsible for the ultimate load of a beam with a large opening.

4.1 The distribution of the shear force

Figure 8 gives consolidated findings about the ultimate load and the cause of failure as well as about the contingent of the shear force of the compression chord at each level of loading. The M/V -ratio has been varied while the quantity of reinforcement has been held constant ($A_{s2}=A_{s3}=A_{s4}=2,26$ cm², $A_{s1}=9,82$ cm²).

Focusing on the ultimate load we can recognize that the ultimate load decreases with the M/V -ratio. For high M/V -ratios ($M/V \geq 1,0$ m) which correspond with openings at the beam's midspan the longitudinal reinforcement of the tension chord fails because of the magnitude of the global moment. Of course this effect also reduces the ultimate load. In all other cases the fourth plastic hinge arises and defines the failure.

Likewise the development of the shear force distribution is strongly affected by the location of the opening. If there is no real tension chord ($M/V \leq 0,50$ m) the reinforcement's magnitude determines the shear force distribution on the chords. Only in beams with openings further away from the support the compression chord gets the most quantity of the total shear force V_{tot} . This will reach up until 80 %.

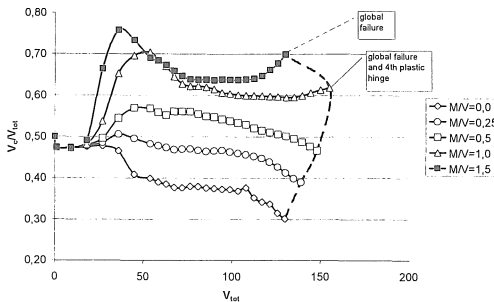


Figure 8. Shear force distribution for $\alpha_t=0,19$

If the ratio M/V is kept constant on the small level of 0,5 m and only the magnitude of A_{s1} is varied the results presented in figure 9 can be expected.

The maximum ultimate load is reached at the fourth plastic hinge if the tension chord's reinforcement A_{s1} is very large in comparison to the other reinforcement layers. The magnitude of A_{s1} also affects the distribution of the shear force at the level of the ultimate load and during the loading phase. The higher the quantity of A_{s1} is the smaller is the compression chord's contingent of the shear force. The reinforcement's magnitude shows stronger effects for small M/V -ratios than for higher ones. As we will see later this will have consequences for the formation of the first plastic hinge.

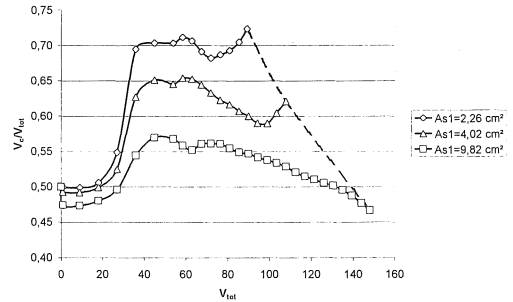


Figure 9. Shear force distribution for $M/V=0,5$ m

4.2 The contraflexure point in the tension chord

Almost every researcher in the past has assumed that the contraflexure points of the beam's chords which represent the point of $M=0$ kNm are located at the midspan of the chords. Mansur et al. (1985) pointed out that the location of the contraflexure points depends on the value of α_t . They suggest that for symmetrically reinforced chords ($\alpha_t=0,5$) the location of the contraflexure points at the chord's midspan. For unsymmetrically reinforced chords ($\alpha_t < 0,5$) the inflection point does not occur at the midpoint. In most cases this is the tension chord. In their measurements they could determine just negligible eccentricities, which could be disregarded in the most analytical approaches in their opinion.

The evaluation of the comprehensive FE-studies ensured by the measurements we did at our experiments in the past lead to the following results. The location of the contraflexure points are found if an approximated function for the chord's deflection in $u(x)=f(x^3)$ is identified. By deriving $u(x)$ twice and solving $u''(x)=0$ the result is l_E .

It is obvious that the magnitude of the eccentricity of the contraflexure point l_E depends on the rein-

forcement's ratio as well as on the system of loads represented by M/V . The influence of the system of loads can be simply illustrated by a picture of the deformation due to pure bending (fig. 10). The deformation of the global system due to bending moments indicates constant bending moments in the chord members.



Figure 10. Deformation of the chords due to pure bending

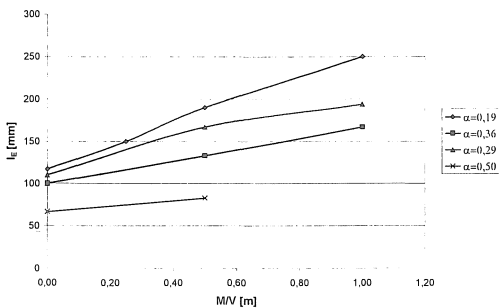


Figure 11. Magnitude of l_E due to M/V

This leads to increasing eccentricities of the contraflexure point l_E for increasing M/V -ratios (fig. 11). In every case l_E is unequal to zero even for $M/V=0,0$ m and $\alpha_t=0,50$. The reason for this is that the global bending moment M is just equal to zero at the midpoint of the opening. At the ends of the opening's chords the bending moment is always unequal to zero. Just the difference between the magnitude of M from each end of the opening to the other can be modified. However, a system where M equals zero along the whole length of the opening does not exist. Consequently l_E is always unequal to zero because of the different fixed supports of the chords' ends.

As expected from Mansur's findings (Mansur et al. 1985) the evaluation of the deflection curves of unsymmetrically reinforced chords represented by α_t shows the eccentricity of the contraflexure point (fig. 12).

5 PROPOSAL FOR A NEW DESIGN CONCEPT

As shown in chapter 4 the load bearing behaviour is strongly affected by the magnitude of the reinforcement in the chords and the combination of loadings

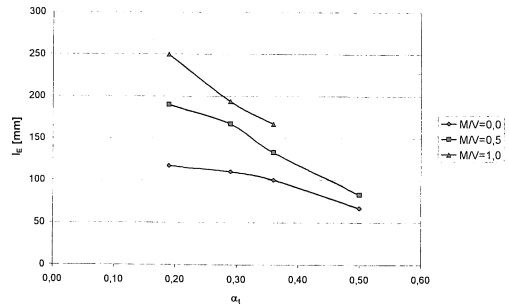


Figure 12. Magnitude of l_E due to α_t

represented by M/V . If the opening's location and dimensions have been determined in statically determinated systems the global internal forces at the midspan of the opening are known. The internal forces of the vierendeel panel at the opening can be determined almost exactly if the magnitude of the reinforcement of the chords is estimated. By ignoring the eccentricity of the contraflexure points at this time a very good estimation of the shear force distribution can be done by using figure 13. With its help the reinforcement's quantity can be estimated roughly.

Afterwards a more detailed and economic design process can be started by the determination of the shear force distribution at three characteristic load levels until the first plastic hinge arises in point 3 of figure 14. This happens in almost every case when the reinforcement A_{s2} reaches its tensile strength. Exceptions are beams with little reinforcement in the tension chord and small M/V -ratios. The consideration of the eccentricity of the contraflexure point in the tension chord leads to that system of loads which characterizes the ultimate limit state. Completing the evidence of the load bearing capacity of the chord members has to be proven by using M-N-interaction diagrams which will be developed for unsymmetrically reinforced chords.

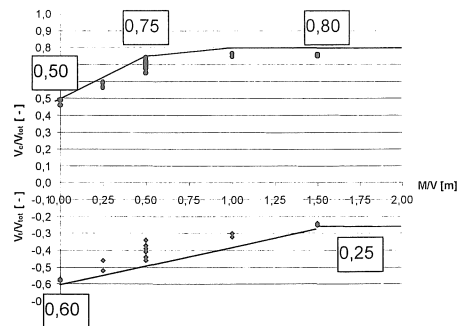


Figure 13. Estimating the shear force distribution for rectangular beams with $l_1/l_c=1,0$ (Krips 2001)

5.1 Determination of the shear force distribution

The evaluation of the shear force distribution can be visualized in figure 14 very vividly. The evaluation can be subdivided into five characteristic steps, while four of them can be determined appropriately:

5.1.1 Step 1

The shear force distribution is determined by the ideal flexure stiffnesses until cracks in the tension chord appear.

5.1.2 Step 2

If no cracks are present in the compression chord all additional shear forces during loading period 2 are carried by the compression chord. This observation coincides with the results of Hanson (1969).

5.1.3 Step 3

During this loading period the additional shear forces are distributed like the ratio of the chords' stiffnesses in the cracked state changes. Just before cracks in the compression chord are found the flexural stiffness of the tension chord amounts to:

$$I_{t,2} = \frac{V_t}{V_c} \cdot I_{c,2} \quad (2)$$

At point 3 in figure 14 in almost every case it can be assumed that the tension chord shows cracks over its whole length. Then the tension chord's flexural stiffness can be determined by the reinforcement only. In point 2 no cracks are present in the compression chord and the ideal stiffness has to be used. The flexural stiffness at the ends of the compression chord in point 3 can be determined via the shear force distribution given in figure 13. With the use of the M-N-interaction diagram in figure 15 the load bearing capacity of the tension chord's ends can be determined. Point 3 with the first plastic hinge is fixed. At the midspan of the compression chord it can be assumed that there are no cracks. Based on this a substitution of the flexural stiffness of the compression chord can be derived.

The evaluation of all performed tests shows that the shear force distribution during loading period 3 amounts in ratio to the variations of the chords' flexural stiffnesses about 0,50. Except if the magnitude of the reinforcement in the tension chord is twice as high as the one in the compression chord the ratio of the shear force distribution amounts to $V_c/V_{tot}=0,40$ during this loading period.

5.1.4 Step 4

The load bearing capacity respectively the formation of the first plastic hinge occurs later than defined by point 3 because of the eccentricity of the contraflexure point in the tension chord (point 4*). This effect can be taken into consideration by using

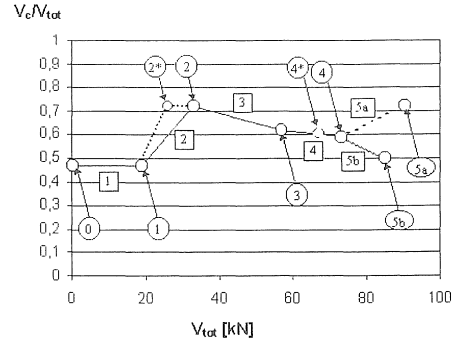


Figure 14. Outline of the evaluation of the shear force distribution (Kripos 2001)

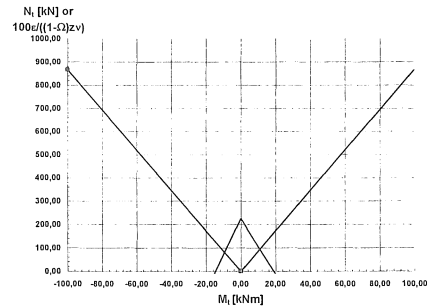


Figure 15. Outline of an M-N-interaction diagram for the determination of the first plastic hinge

figure 15. In point 4 the second plastic hinge arises.

5.1.5 Step 5

During this loading period which is characterized by the formation of the last two plastic hinges an exact quantity of the shear force distribution cannot be predicted. Additionally there is a risk that the deflections at the serviceability limit state become too large.

5.2 Determination of the contraflexure point

As shown in chapter 4 the location of the contraflexure point is strongly affected by the ratio of M/V and the unsymmetrically reinforced chords. The eccentricity l_E can be characterized appropriately by the following equation:

$$l_E = 150 - 164 \cdot \alpha_t + 67 \cdot \frac{M}{V} \quad (3)$$

In figure 16 it can be recognized that a proper conformity appears by the suggested proceeding to determine the shear force distribution and the ex-

centricity of the contraflexure point in the tension chord.

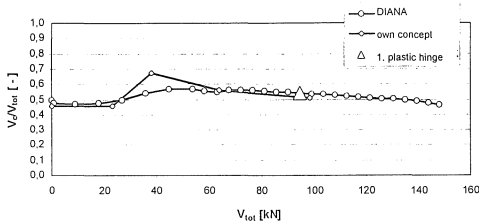


Figure 16. Comparing the new determined concept with DIANA-results

6 CONCLUDING REMARKS AND FUTURE WORK

In this short survey of the latest research results it could be shown that two new parameters have to be taken into consideration when dealing with reinforced concrete beams with large openings. Openings close to the supports can be handled with respect to a detailed computation of the shear force distribution on the chords. The influence of an excentric location of the contraflexure point in the tension chord should be taken into account in order to obtain proper and economic results i. e. an economic amount of reinforcement. The ultimate load characterized by the formation of the first plastic hinge can be determined reliably. Further considerations to increase the ultimate load should be avoided since the prediction of the shear force distribution becomes unreliable. Additionally it can be assumed that in many cases the first plastic hinge arises before the serviceability limit state.

For the ongoing work it is planned to transfer the design concept to different geometrical dimensions of the concrete beam's chords. Therefore a huge series of T-beams has already been computed with DIANA.

In another step of the research project which has been promoted by the German Science Foundation (DFG) since January 2000 the deflection of beams with openings in contrast to massive beams will be checked and evaluated. Further computations using the discrete cracking concept are supposed to generate information about the crack width and if necessary suitable proposals for dimensions and forms of reinforcement at the opening's corners.

By the performance of the prepared test program with common dimensions in our laboratory the confirmation of the theoretical findings is expected.

REFERENCES

- CEB-FIP Model Code 1990. CEB Bulletin d'Information. Design Code. Lausanne.
- Dilger, W. 1966. *Veränderlichkeit der Biege- und Schubtragfähigkeit bei Stahlbetontragwerken und ihr Einfluß auf die Schnittkraftverteilung und Traglast bei statisch unbestimmter Lagerung*. DAFStb. Heft 179. Berlin: Verlag Ernst & Sohn.
- Ehmann, S. & Pfeffer, K. & Schnellenbach-Held, M. 1999. Computational Modeling of Reinforced Concrete Structures with DIANA. *Darmstadt Concrete*. Annual journal on concrete and concrete structures. Vol. 14: 37-48.
- Eligehausen, R. & Gerster, R. 1993. *Das Bewehren von Stahlbetonbauteilen*, DAFStb. Heft 399. Berlin: Verlag Ernst & Sohn.
- Hanson, J. M. 1969. Square Openings in Webs of Continuous Joists. Informal Report. Chicago: Portland Cement Association.
- Hordijk, D. A. 1992. *Tensile and Tensile Fatigue Behaviour of Concrete*. Experiments, Modelling and Analyses. HERON 71 (1). Delft.
- Kripi, E. 2001. *Zur Verteilung der Querkraft auf Druck- und Zuggurt bei Balken mit großen Öffnungen*. Diploma thesis. Institut für Massivbau. TU Darmstadt.
- Leonhardt, F. 1977. *Vorlesungen über Massivbau*. Dritter Teil. Grundlagen zum Bewehren im Stahlbetonbau. Berlin: Springer Verlag.
- Lorentsen, M. 1962. Holes in Reinforced Concrete Girders. Informal Report. Chicago: Portland Cement Association.
- Mansur, M. A. & Tan, K. H. 1999. *Concrete Beams with Openings. Analyses and Design*. Boca Raton London New York Washington D. C.: CRC Press.
- Mansur, M. A. & Tan, K. H. & Lee, S. L. 1985. Design Method for Reinforced Concrete Beams with Large Openings. *ACI Journal* 82 (46): 517-524.
- Nasser, K. W. et al. 1967. Behaviour and Design of Large Openings in Reinforced Concrete Beams. *ACI-Journal* 1.67: 25-33.
- Reit, H.-G. 1994. *Untersuchungen zum Interaktionsverhalten von Stahlbetonbalken unter Biegemomenten-, Querkraft- und Normalbeanspruchung*. Dissertation. Universität Kaiserslautern.
- Tan, K. H. 1982. *Ultimate Strength of Reinforced Concrete Beams with Rectangular Openings under Bending and Shear*. Master thesis. National University of Singapore.
- Vecchio, F. J. & Collins, M. P. 1986. The Modified Compression Field Theory for Reinforced Concrete Elements Subjected to Shear. *ACI Journal* 83 (22): 219-231.
- Wommelsdorf, O. 1993. *Stahlbetonbau*. Bemessung und Konstruktion. Teil 2. Düsseldorf: Werner-Verlag GmbH.